Physiological FDG uptake in growth plate on pediatric PET

AUTHOR(S):

Otani, Tomoaki; Nakamoto, Yuji; Ishimori, Takayoshi

CITATION:

Otani, Tomoaki ...[et al]. Physiological FDG uptake in growth plate on pediatric PET. Asia Oceania Journal of Nuclear Medicine & Biology 2021, 9(1): 15-20

ISSUE DATE:

2021-01

URL:

http://hdl.handle.net/2433/277832

Asia Oceania Journal of Nuclear Medicine & Biology
http://aojnmb.mums.ac.ir
AOJNMB

Physiological FDG uptake in growth plate on pediatric PET

Tomoaki Otani, Yuji Nakamoto*, Takayoshi Ishimori

Department of Diagnostic Imaging and Nuclear Medicine, Graduate School of Medicine, Kyoto University, Japan

ARTICLEINFO

Article type:
Original Article

Article history:
Received: 17 Jun 2020
Revised: 12Aug 2020
Accepted: 29Aug2020

Keywords:
Growth plate
Physiological FDG uptake
FDG

ABSTRACT

Objective(s): ^{18}F-Fluorodeoxyglucose (FDG) uptake in children is different from that in adults. Physiological accumulation is known to occur in growth plates, but the pattern of distribution has not been fully investigated. Our aim was to evaluate the metabolic activity of growth plates according to age and location.

Methods: We retrospectively evaluated 89 PET/CT scans in 63 pediatric patients (male : female=25 : 38, range, 0–18 years). Patients were classified into four age groups (Group A: 0–2 years, Group B: 3–9 years, Group C: 10–14 years and Group D: 15-18 years). The maximum standardized uptake value (SUV_{max}) of the proximal and distal growth plates of the humerus, the forearm bones and the femur were measured. The SUV_{max} of each site and each age group were compared and statistically analyzed. We also examined the correlations between age and SUV_{max}.

Results: As for the comparison of SUV_{max} in each location, the SUV_{max} was significantly higher in the distal femur than those in the other sites ($p< 0.01$). SUV_{max} in the distal humerus and the proximal forearm bones were significantly lower than those in the other sites ($p< 0.01$). In the distal femur, there was large variation in SUV_{max}, while in the distal humerus and the proximal forearm bones, there was small variation. As for the comparison of SUV_{max} in each age group, the SUV_{max} in group D tended to be lower than those in the other groups, but in the distal femur, there was no significant difference among each age group.

Conclusion: Our data indicate that FDG uptake in growth plates varies depending on the site and age with remarkable uptake especially in the distal femur.

Please cite this paper as:

Otani T, Nakamoto Y, Ishimori T.Physiological FDG uptake in growth plate on pediatric PET. Asia Ocean J Nucl Med Biol. 2021; 9(1): 15-20. doi: 10.22038/AOJNMB.2020.49638.1339

Introduction

^{18}F-Fluorodeoxyglucose-positron emission tomography/computed tomography (PET/CT) is well established as a functional imaging tool for diagnosis, staging, and therapeutic response monitoring in many malignant diseases, and is also being applied with increasing frequency in the management of various malignancies in children (1,2). Physiological FDG uptake in children is unique and is somewhat different to that in adults in some regions or organs. To interpret PET images properly and to distinguish between physiological uptake and abnormal uptake, it is important to know the pattern, intensities, and frequencies of physiological FDG distribution. There are several reports regarding physiological uptake in pediatric PET/CT for regions such as head and neck, thymus, spinal cord, and bone marrow (3-6).

There are two different types of bone growth, membranous ossification and endochondral ossification. Growth plates are the site of endochondral ossification, in which cartilage is first formed and remodeled into bone tissue and are responsible for longitudinal bone growth (7). In bone scintigraphy, several studies have shown that increased tracer uptake can occur in the growth plates in response to conditions that affect metabolic activity in the skeleton; e.g.,trauma or infection (8, 9) and bone scintigraphy was a useful tool for the evaluation and follow-up of growth and development in children (10). In addition, Yamane et al. revealed that the SUV was increased at the growth plates of children under the age of 15 years in comparison with the older patients (11).

Physiological accumulation of FDG in growth plates is also reported (12). However, the pattern

* *Corresponding author:* Yuji Nakamoto. Department of Diagnostic Imaging and Nuclear Medicine, Graduate School of Medicine, Kyoto University, 54 Shogoinkawahara-cho, Sakyo-Ku, Kyoto 606-8507, Japan.Tel: +81-75-751-3760; Fax: +81-75-771-9709;Email: ynakamo1@kuhp.kyoto-u.ac.jp

of distribution in the growth plates has not been fully investigated for PET/CT, so the normal patterns of FDG uptake need to be revealed in a broad population. The aim of this retrospective study was to evaluate the metabolic activity of the growth plates according to age and location and to establish normal uptake pattern in growth plates.

Methods

Patients

This study received approval from the ethics committee of our institute. Because of the anonymous nature of the data and the retrospective study design, the requirement for written informed consent was waived, but written informed consent was obtained for data access before scanning. We retrospectively evaluated 89 consecutive PET/CT scans in 63 pediatric patients (male: female= 25:38, range, 0-18 years) who underwent PET/CT for follow-up after treatment of malignant tumor without recurrence or for evaluation of suspected cancer without evidence of malignancy between June 2009 and March 2020. Patients with malignant and active inflammatory disease were excluded since they were arguably in a state of physiologic stress and the uptake of bone marrow could be altered. In addition, patients with history of previous craniospinal radiotherapy were excluded since craniospinal irradiation has negative impact on growth (13). We analyzed five patients for each age except in patients with the age of less than 3 years old because less than 5 cases met the criteria in our database, i.e. 0-year-old: 3 cases, 1-year-old: 3 cases, 2-year-old: 4 cases, and 3-year-old: 4 cases. Of the 63 patients, 19 were follow up after treatment of hematologic disorder, 6 for post-transplantation lymphoproliferative disorder (PTLD), 3 for liver tumor, 3 for teratoma and 16 for other diseases. Sixteen patients were suspected malignant disease, but no malignant disease was presented. More than one year have passed since the last treatment completed in patients with malignancy.

^{18}F-FDG PET/CT scanning

PET/CT scans were performed on two dedicated PET/CT scanners (Discovery ST Elite GE Healthcare, Waukesha, WI, n=27; Discovery IQ, 5-ring detector configuration, GE Healthcare, n=62). No harmonization was done between the two scanners. After fasting for at least 4 h, all patients received intravenous injection of 27.3–346.1 MBq of FDG according to the consensus guidelines of our country for pediatric nuclear medicine (14). According to these guidelines, the administered dose is calculated using baseline activity (14 MBq) and a weight-dependent multiple. PET emission data were acquired at 65 min (median, interquartile range 59-70 min) post injection. The scanning range was from the top of the skull to the mid-thigh or toe for 2–3 min per bed position. Low-dose CT was acquired of the same areas. The CTDIvol of the low-dose CT was 0.30–1.60. The CT data were used for attenuation correction, and images were reconstructed using an ordered-subset expectation maximization (OSEM) -based algorithm (2 iterations and 14 subsets for Discovery ST Elite, and 4 iterations and 12 subsets for Discovery IQ).

Image analysis

All PET/CT images were reviewed on a dedicated workstation (Advantage Workstation v.4.6: GE Healthcare). PET/CT images were analyzed qualitatively by one board-certified radiologist. The linear accumulation found in epiphysis was regarded as the accumulation in growth plate. Spherical volume of interest (VOI) was placed manually on the proximal and distal growth plates of the humerus, the forearm bones (radius and ulna), and the femur. The VOIs were placed on the right and left separately. The maximum standardized uptake value (SUV_{max}) in growth plate was measured in each VOI. Referring to the previous report (15), the patients were divided into four groups according to age: Group A (infant), 0–2 years (median age 1.0 yr, n=10); Group B (juvenile), 3–9 years (median age 6.0 yr, n=34); Group C (early-adolescent), 10–14 years (median age 12.0 yr, n=25); Group D (delay-adolescent), 15-18 years (median age 16.5 yr, n=20). The SUV_{max} of each site and each age were compared and statistically analyzed. We also examined the correlations between age and SUV_{max}.

Statistical analysis

All statistical analyses were performed with JMP (version 14.1.0 SAS Institute, Cary, NC). A p value<0.05 was considered statistically significant. The Steel-Dwass test was used for the multiple comparison of SUV_{max} at each site and in each age group.

Results

Relation between SUV_{max} and age / gender

The scatter plots in Figure 1 shows the relationship between age and SUV_{max} according to location. In the distal femur, there was large variation in SUV_{max}, while in the distal humerus and the proximal forearm bones, there was small variation. Table 1 shows the median and interquartile range of SUV_{max} at each site for each age. Table 2 shows the median and interquartile

range of SUV_{max} at each site for each age according to gender. In Group C and D (10-18 years), the median values in female reached the peak at younger age than in male in the proximal humerus, the distal forearm bones, the proximal and distal femur, but it was not observed in the distal humerus and the proximal forearm bones.

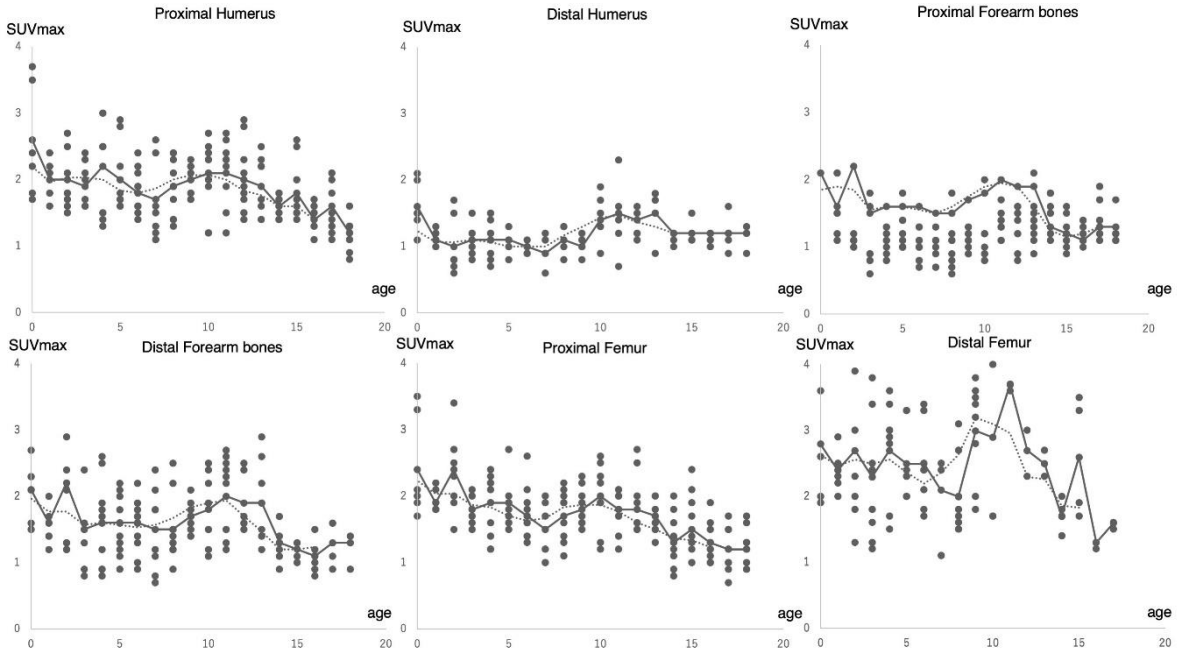

Figure 1. Scatter plot demonstrating the relationship between age and SUV_{max} according to location. The solid lines show the average value of SUV_{max} for each age, and the dotted lines demonstrate the moving median lines of three years

Table 1. SUV_{max} for each age and location (median, interquartile range)

	Proximal humerus	Distal humerus	Proximal forearm bones	Distal forearm bones	Proximal femur	Distal femur
18	1.2, 1.1-1.3	1.2, 1.0-1.3	1.2, 1.1-1.2	1.2, 0.9-1.4	1.2, 1.0-1.4	NA
17	1.5, 1.3-2.0	1.2, 1.1-1.3	1.3, 1.1-1.4	1.4, 1.0-1.6	1.1, 1.0-1.5	1.6, 1.5-1.6
16	1.5, 1.3-1.6	1.1, 1.1-1.2	1.2, 1.0-1.4	1.1, 0.9-1.3	1.2, 1.0-1.5	1.3, 1.2-1.3
15	1.7, 1.5-2.1	1.2, 1.1-1.3	1.2, 1.2-1.3	1.2, 1.0-1.3	1.4, 1.2-2.0	2.6, 1.8-3.5
14	1.6, 1.4-1.7	1.2, 1.1-1.2	1.2, 1.1-1.6	1.3, 1.1-1.5	1.3, 1.1-1.7	1.7, 1.4-1.9
13	2.1, 1.6-2.2	1.5, 1.3-1.8	1.5, 1.3-1.8	1.7, 1.4-2.5	1.7, 1.5-1.9	2.5, 2.3-2.7
12	1.9, 1.5-2.4	1.4, 1.2-1.5	1.5, 1.4-1.6	1.7, 1.6-2.4	1.6, 1.5-2.1	2.7, 2.3-3.0
11	2.3, 1.8-2.5	1.5, 1.1-1.8	1.3, 1.1-1.6	2.3, 1.5-2.5	1.9, 1.6-2.0	3.7, 3.6-3.7
10	2.2, 1.7-2.4	1.2, 0.9-1.4	1.3, 1.2-1.5	1.7, 1.3-2.4	2.0, 1.8-2.4	2.9, 1.7-4.0
9	2.1, 1.8-2.2	1.1, 0.9-1.2	1.0, 0.9-1.2	1.7, 1.5-1.8	1.7, 1.6-2.1	3.3, 2.2-3.6
8	1.9, 1.4-2.3	1.1, 1.0-1.2	1.2, 1.0-1.2	1.4, 1.2-1.7	1.8, 1.3-2.0	1.8, 1.5-2.5
7	1.6, 1.2-2.1	0.9, 0.7-1.1	0.9, 0.7-1.1	1.5, 1.0-1.9	1.5, 1.2-1.8	2.5, 1.1-2.7
6	1.8, 1.6-2.1	1.0, 0.9-1.1	1.1, 1.0-1.1	1.7, 1.2-1.8	1.7, 1.4-2.0	2.4, 1.9-3.1
5	1.8, 1.7-2.4	1.1, 1.0-1.2	1.0, 1.0-1.2	1.5, 1.0-1.6	1.8, 1.6-2.2	2.3, 2.0-3.1
4	2.5, 1.5-2.6	1.2, 0.9-1.4	1.3, 1.0-1.4	1.7, 0.9-2.1	2.0, 1.4-2.2	3.0, 2.0-3.3
3	1.9, 1.6-2.3	1.1, 0.9-1.2	1.1, 0.9-1.2	1.5, 1.0-1.6	1.8, 1.6-2.0	2.1, 1.4-3.2
2	1.8, 1.6-2.4	0.8, 0.7-1.3	1.0, 0.8-1.5	1.7, 1.2-2.8	2.4, 1.9-2.7	2.5, 1.9-3.7
1	2.1, 1.8-2.3	1.1, 1.1-1.2	1.1, 1.1-1.1	1.5, 1.4-1.8	1.9, 1.8-2.1	2.4, 2.2-2.6
0	2.3, 1.8-3.6	1.5, 1.3-2.0	1.5, 1.2-2.1	2.2, 1.6-2.4	2.1, 1.9-3.4	2.6, 2.0-3.7

Table 2. SUV_{max} for each age and location according to gender (median, interquartile range). Bold type indicates the highest value in median of SUV_{max} in Group C and D (10-18 years)

	Proximal humerus		Distal humerus		Proximal forearm bones		Distal forearm bones		Proximal femur		Distal femur	
	Male	Female	Male	Female	Male	Female	Male	Female	Male	Female	Male	Female
18	1.3, 1.0-1.5	1.3, 1.2-1.3	1.1, 1.0-1.2	1.2, 1.0-1.4	NA	1.2, 1.1-1.2	NA	1.2, 0.9-1.4	1.1, 0.9-1.3	1.3, 1.2-1.6	NA	NA
17	1.6, 1.2-2.0	1.5, 1.4-1.5	1.2, 1.1-1.4	1.2, 1.1-1.2	1.3, 1.1-1.4	1.3, 1.3-1.3	1.4, 1.0-1.6	NA	1.4, 0.9-1.5	1.0, 1.0-1.0	1.6, 1.5-1.6	NA
16	1.5, 1.3-1.7	1.5, 1.3-1.5	1.1, 0.9-1.3	1.2, 1.1-1.3	1.1, 1.0-1.2	1.3, 1.0-1.5	1.2, 1.0-1.4	0.9, 0.8-0.9	1.1, 1.0-1.3	1.4, 1.1-1.7	NA	1.3, 1.2-1.3
15	2.0, 1.5-2.6	1.7, 1.5-2.0	1.4, 1.1-1.7	1.1, 1.1-1.2	1.3, 1.2-1.6	1.2, 1.1-1.2	1.1, 1.0-1.1	1.3, 1.3-1.3	1.8, 1.3-2.3	1.3, 1.0-1.8	1.8, 1.7-1.9	3.4, 3.3-3.5
14	1.5, 1.4-1.6	1.7, 1.4-1.8	1.1, 1.0-1.2	1.2, 1.1-1.2	1.2, 1.1-1.2	1.2, 1.2-1.8	1.0, 0.9-1.1	1.4, 1.2-1.6	1.2, 1.1-1.2	1.4, 1.0-1.8	1.8, 1.7-1.8	1.6, 1.4-1.9
13	2.2, 2.0-2.4	1.7, 1.4-2.2	1.6, 1.4-1.8	1.5, 0.9-1.8	1.6, 1.3-1.8	1.5, 1.1-1.7	1.7, 1.4-2.1	2.0, 1.3-2.8	1.6, 1.4-1.7	1.8, 1.6-2.0	2.5, 2.3-2.7	NA
12	2.5, 1.7-2.9	1.8, 1.5-2.0	1.3, 1.1-2.0	1.4, 1.2-1.5	1.5, 1.3-2.0	1.5, 1.4-1.5	2.1, 1.6-2.5	1.6, 1.6-1.6	2.3, 1.9-2.7	1.6, 1.5-1.6	2.7, 1.9-3.7	NA
11	2.3, 2.3-2.3	1.8, 1.5-2.0	2.1, 1.9-2.3	1.4, 0.9-1.6	1.6, 1.5-1.7	1.2, 1.0-1.5	2.5, 2.2-2.7	1.9, 1.4-2.5	2.0, 2.0-2.0	1.8, 1.5-2.1	NA	3.7, 3.6-3.7
10	1.6, 1.2-2.0	2.4, 2.2-2.6	1.1, 0.9-1.4	1.5, 1.3-1.9	1.2, 1.1-1.4	1.4, 1.3-1.9	1.4, 1.1-1.5	2.3, 2.0-2.5	1.6, 1.2-2.0	2.3, 1.9-2.5	1.7, 1.7-1.7	4.0, 4.0-4.0
9	1.9, 1.7-2.2	2.1, 1.8-2.2	1.1, 1.0-1.2	1.0, 0.8-1.2	1.2, 1.0-1.3	0.9, 0.8-1.0	1.6, 1.4-1.9	1.7, 1.5-1.9	1.8, 1.6-2.0	1.7, 1.6-2.2	2.8, 1.9-3.7	3.3, 2.9-3.6
8	2.4, 2.2-2.4	1.6, 1.4-1.9	1.2, 1.0-1.3	1.1, 0.8-1.1	1.2, 1.1-1.3	1.1, 0.9-1.4	1.7, 1.0-2.4	1.4, 1.2-1.5	2.0, 1.9-2.2	1.4, 1.1-1.7	2.2, 1.6-3.0	1.7, 1.5-2.0
7	NA	1.6, 1.2-2.1	NA	0.9, 0.7-1.1	NA	0.9, 0.7-1.1	NA	1.5, 1.0-1.9	NA	1.5, 1.2-1.8	NA	2.5, 1.1-2.7
6	1.8, 1.6-1.9	1.8, 1.5-2.2	1.1, 1.0-1.1	1.0, 0.9-1.1	0.9, 0.7-1.1	1.1, 1.0-1.1	1.8, 1.7-1.8	1.5, 1.1-1.9	1.7, 1.6-1.7	1.7, 1.4-2.1	3.4, 3.3-3.4	2.3, 1.8-2.4
5	1.9, 1.7-2.7	1.7, 1.6-1.8	1.1, 1.0-1.2	1.0, 0.8-1.2	1.1, 1.0-1.3	0.8, 0.7-0.8	1.7, 1.2-2.1	1.2, 0.9-1.4	1.8, 1.6-2.5	1.7, 1.6-1.8	2.4, 2.0-3.3	2.2, 2.0-2.3
4	2.4, 2.4-3.0	1.5, 1.3-1.5	1.2, 1.1-1.4	0.9, 0.7-1.4	1.3, 1.2-1.5	0.9, 0.8-1.3	1.9, 1.7-2.5	0.9, 0.8-1.1	2.2, 2.1-2.3	1.3, 1.2-1.6	3.0, 2.9-3.5	1.6, 1.5-1.7
3	1.9, 1.6-2.0	2.0, 1.6-2.4	1.0, 0.8-1.1	1.2, 1.1-1.4	1.0, 09-1.1	1.2, 1.0-1.2	1.2, 0.8-1.6	1.6, 1.4-2.2	2.0, 1.9-2.1	1.7, 1.5-1.7	1.9, 1.2-2.5	2.6, 1.7-3.7
2	NA	1.8, 1.6-2.4	NA	0.8, 0.7-1.3	NA	1.0, 0.8-1.5	NA	1.7, 1.2-2.8	NA	2.4, 1.9-2.7	NA	2.5, 1.9-3.7
1	NA	2.1, 1.8-2.3	NA	1.1, 1.1-1.2	NA	1.1, 1.1-1.1	NA	1.5, 1.4-1.8	NA	1.9, 1.8-2.1	NA	2.4, 2.2-2.6
0	1.8, 1.7-1.8	3.0, 2.3-3.7	1.3,1.1-1.4	1.8, 1.5-2.1	1.2, 1.1-1.2	1.8, 1.5-2.1	1.6, 1.5-1.6	2.3, 2.2-2.6	1.8, 1.7-1.9	2.7, 2.0-3.5	2.0, 1.9-2.0	3.1, 2.6-4.0

Comparison of SUV_{max} in each age group

Figure 2 shows representative maximum-intensity-projection (MIP) PET images for each age group. The SUV_{max} for each age group and location are summarized in Figure 3. In the proximal humerus and the distal forearm bones, the SUV_{max} in Group D was significantly lower than those in the other groups ($p<0.01$). In the distal humerus and the proximal forearm bones, the SUV_{max} in Group C was significantly higher than those in Group B and Group D ($p<0.01–0.03$) and the SUV_{max} in Group D was significantly higher than that in Group B ($p<0.01$). In the proximal femur, the SUV_{max} in Group D was significantly lower than those in the other groups ($p<0.01$) and the SUV_{max} in Group A was significantly higher than those in the other groups ($p<0.01$). In the distal femur, there was no significant difference among each age group ($p=0.15-0.99$).

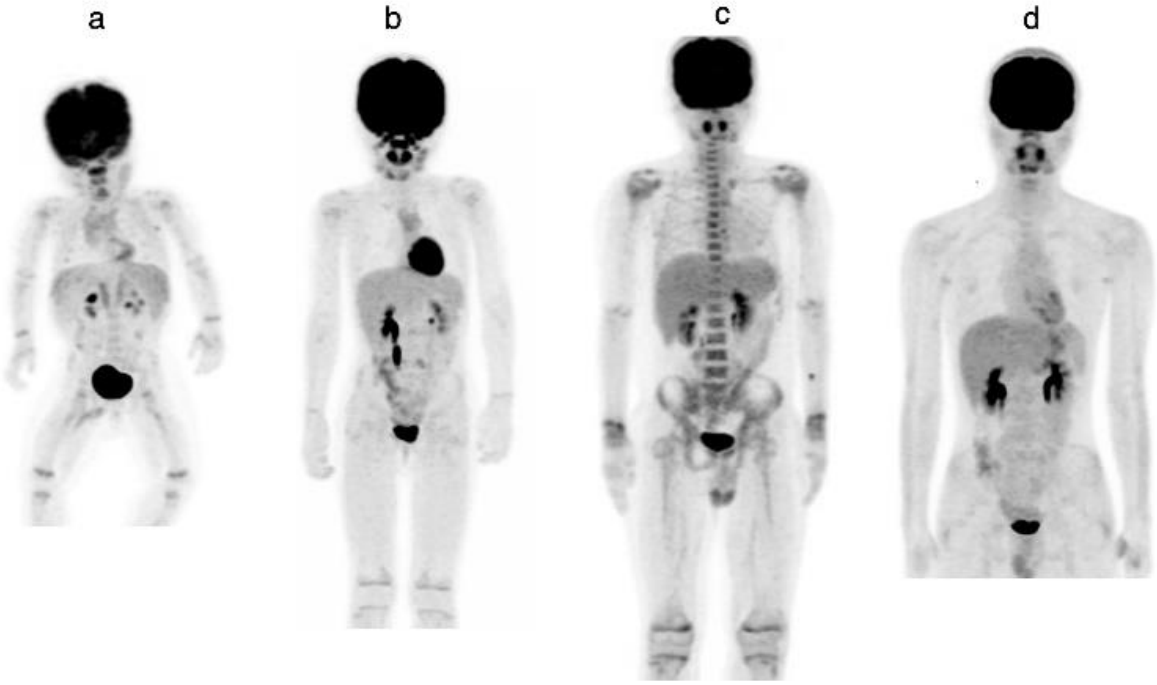

Figure 2. Representative maximum-intensity-projection (MIP) images of each age group. (a) 1-year-old girl, (b) 6-year-old girl, (c) 11-year-old boy and (d) 16-year-old boy. The SUV_{max} values of the proximal and distal growth plates of the humerus, forearm bones, and femur were 1.8/2.0, 1.3/1.1, 1.1/1.2, 2.0/1.6, 1.8/2.1, 2.4/2.5 in patient (a), 1.9/2.0, 1.0/0.9, 0.9/0.9, 1.5/1.8, 1.8/1.9, 2.7/2.9 in patient (b), and 3.3/3.2, 1.7/2.1, 1.7/1.7, 4.2/3.6, 2.3/2.1, 4.3/3.9 in patient (c), and 1.3/1.4, 0.9/1.0, 1.1/1.1, 1.1/1.0, 1.0/1.0 in patient (d) respectively. In patient (d), the distal femur was outside the imaging range

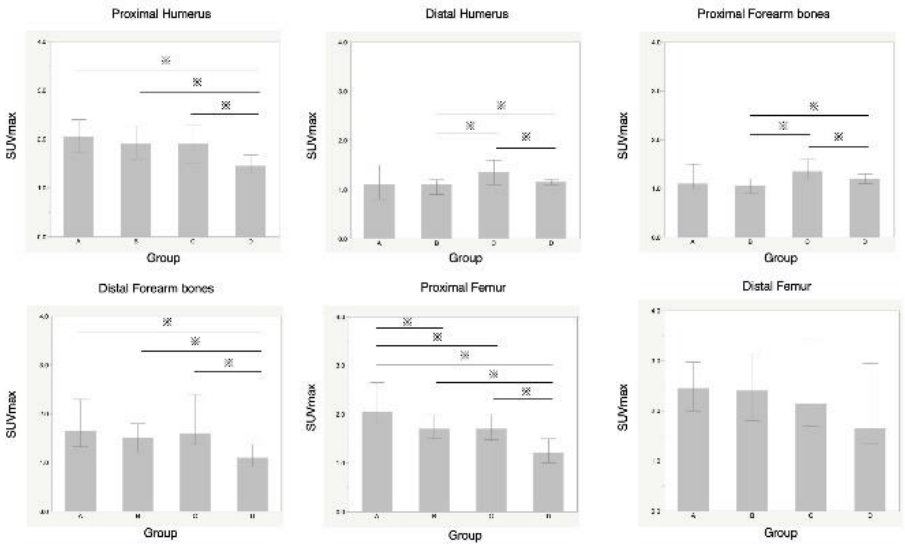

Figure 3. The SUV_{max} for each age group and location. The bar graphs show the median of SUV_{max} and error bars show the interquartile range of SUV_{max}. Group A: 0–2 years, Group B: 3–9 years, Group C: 10–14 years and Group D: 15-18 years
*: $p < 0.05$

Comparison of SUV_{max} in each location

SUV_{max} was significantly higher in the distal femur than those in the other sites ($p<0.01$). SUV_{max} in the proximal humerus was higher than that in the proximal femur ($p=0.03$). There was no significant difference in SUV_{max} between the proximal femur and the distal forearm bones ($p=0.78$). SUV_{max} in the distal humerus and the proximal forearm bones were significantly lower than those in the other sites ($p<0.01$). There was no significant difference in SUV_{max} between the distal humerus and the proximal forearm bones ($p=0.99$).

Discussion

In this retrospective study, we investigated FDG uptake in the growth plates of pediatric patients who were grouped by age and found that uptake varied according to location and tended to be higher in the distal femur. We consider that the variation in FDG accumulation indicates differences in the degree of bone growth associated with endochondral ossification at each site .

It was also revealed that the variation in SUV_{max} was different for each location. In the distal femur, there was large variation in SUV_{max}, while in the distal humerus and the proximal forearm bones, there was small variation, reflecting that there was large variation in the degree of growth in the distal femur, as compared with the distal humerus and the proximal forearm bones.

As for the comparison with SUV_{max} and age group, the SUV_{max} in group D was lower than those in the other groups in the proximal humerus, the distal forearm bones and the proximal femur. It may be related to the closure of the growth plate occurred on average at 14.7 years in female and 16.1 years in male in Japanese(16).

The present study has several limitations. First, the study was retrospective in design, and many of the scans in Group C and D did not include the distal femur. Second, there were only three or four patients for each age of 0 through 3, which may have caused selection bias due to the small number of patients. Third, we did not consider the partial volume effect in this study. It might have affected the uptake in smaller portions, such as the distal humerus, the proximal and distal forearm bones, resulting in lower uptake. Finally, the use of two different PET/CT scanners might have contributed to variability in quantitative values.

Conclusion

Our preliminary data indicate that FDG uptake in growth plates varies depending on location and age, with remarkable uptake especially in the distal femur.

Conflicts of interest and sources of funding

This research did not receive any specific from funding agencies in the public, commercial, or not-for-profit sectors.

References

1. Biermann M, Schwarzlmuller T, Fasmer KE, Reitan BC, Johnsen B, Rosendahl K. Is there a role for PET-CT and SPECT-CT in pediatric oncology? Acta Radiol. 2013; 54(9):1037-45 .
2. Harrison DJ, Parisi MT, Shulkin BL. The Role of (18) F-FDG-PET/CT in Pediatric Sarcoma.

Semin Nucl Med. 2017; 47(3):229-41 .
3. Nakamoto Y, Tatsumi M, Hammoud D, Cohade C, Osman MM, Wahl RL. Normal FDG distribution patterns in the head and neck: PET/CT evaluation. Radiology. 2005;234(3): 879-85.
4. Brink I, Reinhardt MJ, Hoegerle S, Altehoefer C, Moser E, Nitzsche EU. Increased metabolic activity in the thymus gland studied with ^{18}F-FDG PET: age dependency and frequency after chemotherapy. J Nucl Med. 2001; 42(4):591-5.
5. Taralli S, Leccisotti L, Mattoli MV, Castaldi P, de Waure C, Mancuso A, et al. Physiological Activity of Spinal Cord in Children: An ^{18}F-FDG PET-CT Study. Spine (Phila Pa 1976). 2015; 40(11):E647-52 .
6. Jadvar H, Connolly LP, Fahey FH, Shulkin BL. PET and PET/CT in pediatric oncology. Semin Nucl Med. 2007; 37(5):316-31 .
7. Nilsson O, Marino R, De Luca F, Phillip M, Baron J. Endocrine regulation of the growth plate. Horm Res. 2005; 64(4):157-65 .
8. Harcke HT, Mandell GA. Scintigraphic evaluation of the growth plate. Semin Nucl Med. 1993; 23(4):266-73 .
9. Zionts LE, Harcke HT, Brooks KM, MacEwen GD. Posttraumatic tibia valga: a case demonstrating asymmetric activity at the proximal growth plate on technetium bone scan. J Pediatr Orthop. 1987; 7(4):458-62.
10. Celen Z, Zincirkeser S, Ozkilic S, Nacar F. Evaluation of growth in children using quantitative bone scintigraphy. J Int Med Res. 1999; 27(6):286-91 .
11. Yamane T, Kuji I, Sato A, Matsunari I. Quantification of osteoblastic activity in epiphyseal growth plates by quantitative bone SPECT/CT. Skeletal Radiol. 2018; 47(6):805-810.
12. Bestic JM, Peterson JJ, Bancroft LW. Pediatric FDG PET/CT: Physiologic uptake, normal variants, and benign conditions. Radiographics. 2009; 29(5):1487-500.
13. Spoudeas HA. Growth and endocrine function after chemotherapy and radiotherapy in childhood. Eur J Cancer. 2002; 38(13):1748-1759.
14. Koizumi K, Masaki H, Matsuda H, Uchiyama M, Okuno M, Oguma E, et al. Japanese consensus guidelines for pediatric nuclear medicine. Part 1: Pediatric radio-pharmaceutical administered doses (JSNM pediatric dosage card). Part 2: Technical considerations for pediatric nuclear medicine imaging procedures. Ann Nucl Med. 2014; 28(5):498-503 .
15. Karlberg J. On the construction of the infancy-childhood-puberty growth standard. Acta Paediatr Scand Suppl. 1989; 356:26-37.
16. Tanaka T. Bone age atlas for Japanese children. Tokyo: Medical View; 2011.